Basic Reaction Steps in the Sulfidation of Crystalline MoO_3 to MoS_2, As Studied by X-ray Photoelectron and Infrared Emission Spectroscopy

Th. Weber,[†] J. C. Muijsers, J. H. M. C. van Wolput, C. P. J. Verhagen, and J. W. Niemantsverdriet*

Schuit Institute of Catalysis, Eindhoven University of Technology, 5600 MB Eindhoven, The Netherlands

Received: April 25, 1996[⊗]

The sulfidation of crystalline MoO_3 and the thermal decomposition of $(NH_4)_2MoO_2S_2$ to MoS_2 via an $\{MoOS_2\}$ oxysulfide intermediate have been studied by means of monochromatic X-ray photoelectron spectroscopy (XPS) and infrared emission spectroscopy (IRES). Several basic steps of the sulfidation reaction could be resolved and explained in terms of the structure of crystalline MoO_3. The sulfidation reaction starts at low temperatures with an exchange of terminal O^{2-} ligands of the oxide for S^{2-} by reaction with H_2S from the sulfiding atmosphere. In subsequent Mo−S redox reactions, bridging S_2^{2-} ligands and Mo^{5+} centers are formed. Lattice relaxation and further sulfur uptake are the main processes before, at temperatures above 200 °C, direct reactions with H_2 occur, during which the Mo^{5+} centers are converted into the 4+ oxidation state. The decomposition experiments with $(NH_4)_2MoO_2S_2$ show that terminal O^{2-} ligands serve as the reactive sites. The conversion of terminal Mo═O_t to Mo═S entities and the subsequent generation of Mo═O_t from μ_2 and μ_3 oxygen atoms in the MoO_3 lattice appear as the general principle of the sulfidation reaction.

Introduction

Hydrodesulfurization (HDS) of sulfur-containing oil over MoS_2-based catalysts is an increasingly important process, which is utilized in refineries all over the world.[1] HDS catalysts are initially prepared in the form of highly dispersed molybdenum oxides on high-surface-area supports—to which promoters such as Co or Ni may be added—and are subsequently converted into the catalytically active phase by sulfidation, typically in H_2S/H_2 atmospheres at temperatures between 300 and 400 °C:

$$MoO_3 \xrightarrow[H_2S/H_2]{300-400\ ^\circ C} MoS_2 \qquad (1)$$

Being an essential part of the preparation, it is important to know the mechanism of the sulfidation process and to identify the elementary reaction steps. The temperature-programmed studies of Moulijn and co-workers constituted the first systematic approach to the exploration of sulfidation mechanisms.[2,3] Our group has investigated the sulfidation of molybdenum oxide phases in supported model catalysts by surface spectroscopies such as X-ray photoelectron spectroscopy (XPS), secondary ion mass spectrometry (SIMS), Rutherford backscattering spectroscopy (RBS), infrared spectroscopy, and transmission electron microscopy (TEM) by comparison with the chemistry of several Mo−S cluster compounds.[4−6] Although parts of a sulfidation scheme could be identified, a complete mechanism could not yet be proposed, due to the unknown structure of the amorphous oxidic catalyst precursor. The variety of local Mo−O coordination environments, which form in an unpredictable way during the preparation of the catalyst precursor, is the main impediment for understanding the sulfidation reaction. Hence, a study starting from crystalline MoO_3, where elementary reaction steps can be associated with known structural features, is clearly in order.

The purpose of this paper is to describe the sulfidation of crystalline MoO_3, which we investigated with monochromatic XPS and infrared emission spectroscopy (IRES). Both techniques give complementary information on the surface of the particles: XPS reveals the different (oxidation) states of molybdenum and sulfur, while IRES yields valuable information on the changes in Mo−O coordination during sulfidation. As the exchange of oxygen from the MoO_3 lattice with sulfur leads to the formation of oxysulfide phases, it appeared useful to study the thermal decomposition of $(NH_4)_2MoO_2S_2$, in which microcrystalline MoS_2 forms via an $\{MoOS_2\}$ oxysulfide intermediate:[7]

$$(NH_4)_2MoO_2S_2 \rightarrow \{MoOS_2\} + 2NH_3 + H_2O \qquad (2)$$

$$\{MoOS_2\} \rightarrow \text{“}MoS_2\text{”} \qquad (3)$$

Our results combined with literature data on structural, chemical, and spectroscopic properties of Mo−O and Mo−S compounds[5,6,8−11] lead to a mechanistic description of the sulfidation of crystalline MoO_3. We propose a reaction mechanism for reaction 1 in terms of basic reaction steps that either follow from the present work or have known occurrence in the coordination chemistry of molybdenum−oxygen−sulfur compounds.

Experimental Section

Crystalline MoO_3 was used as supplied (Janssen Chimica, 99.999), and $(NH_4)_2MoO_2S_2$ was prepared from a solution of $(NH_4)_6Mo_7O_{24}\cdot 4H_2O$ in NH_4OH and H_2S as described in the literature.[12] The sulfidation experiments were done in a quartz tube reactor. MoO_3 was heated in a flow of 10% H_2S in H_2 (50 mL/min) and kept at the desired temperatures for 3 h, respectively.

XPS spectra were obtained using a VG ESCALAB MK II spectrometer equipped with a monochromatic Al Kα X-ray source and a hemispherical analyzer with a five-channel detector. During measurement the base pressure of the system was around 5×10^{-10} mbar. Spectra were recorded with a constant pass energy of 20 eV. Binding energies were determined by computer fitting the measured spectra. Samples were pressed in indium foil. All steps of the sample preparation were done under inert conditions using a glovebox and a special transport vessel for introducing the samples into the UHV chamber of the spectrometer. Binding energies are estimated to be accurate within ±0.2 eV.

[†] Present address: Laboratories for Technical Chemistry, Swiss Federal Institute of Technology (ETH), CH-8092 Zürich, Switzerland.

* Corresponding author. Fax: +3140-245-5054. E-mail: tgtahn@chem.tue.nl.

[⊗] Abstract published in *Advance ACS Abstracts,* July 15, 1996.

S0022-3654(96)01204-X CCC: $12.00

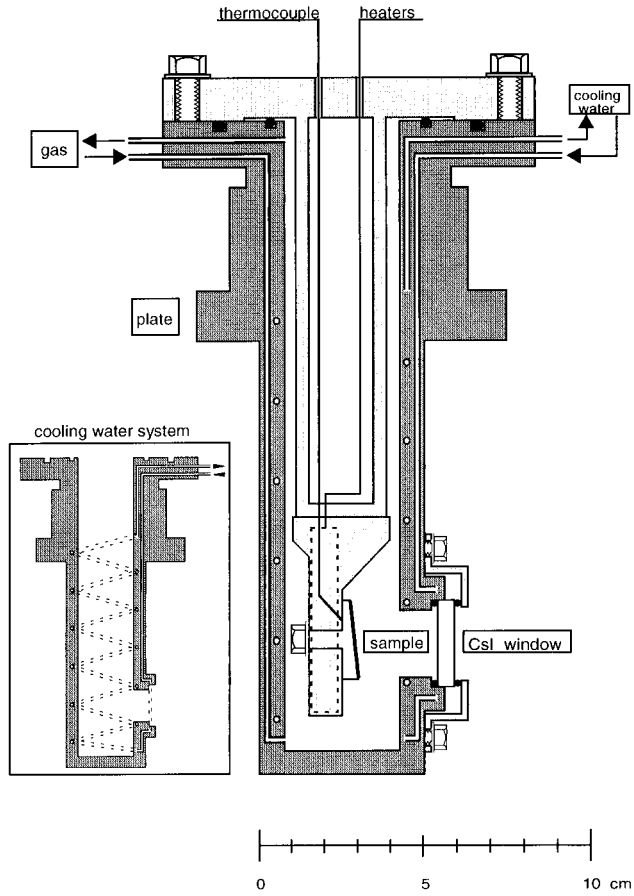

Figure 1. Infrared emission cell (schematic). For explanation see text.

Infrared spectra were obtained with a Bruker IFS 113 v spectrometer equipped with a pyroelectric DTGS detector and with different beam splitters for the far and mid-infrared region. The IR emission studies were done with the emission cell of Figure 1. It consists of two parts. The outer part (dark in Figure 1) is made of aluminum and contains connectors for gases and cooling water. The base plate positions the cell in the spectrometer and closes the source chamber. The window assembly consists of a CsI crystal between two Viton O-rings held together by a flange that is bolted onto the outer part of the cell. The central insert, made of stainless steel, keeps the sample holder and contains connectors for the thermocouple and the heaters. The sample holder is a polished stainless-steel plate on which the sample is prepared as a thin layer. To avoid interferences (leading to low-frequency oscillations in the IR spectra), the surface of the sample holder is tilted. It can be heated to 400 °C, and the temperature can be kept constant within ±0.3 °C. To avoid background emission from the cell, the latter is kept at 18 °C by cooling with water (see box in Figure 1). Sealing is accomplished by Viton O-rings.

The infrared spectrum of $(NH_4)_2MoO_2S_2$ was measured in the absorption mode with a spectral resolution of 4 cm^{-1}. The powdered sample was diluted with CsI and pressed to a self-supporting disk. Spectra taken during the thermal decomposition of $(NH_4)_2MoO_2S_2$ and the sulfidation of MoO_3 were measured in the emission mode with a spectral resolution of 8 cm^{-1} using the infrared emission cell of Figure 1. The samples were applied as thin layers on the surface of the cell as follows. Approximately 2 mg of the sample and 5 mL of 2-propanol were shaken in a vibrating mill. The resulting suspension was spread on the surface of the sample deposition area, the liquid was slowly evaporated, and the sample holder was mounted in the cell. For the thermal decomposition of $(NH_4)_2MoO_2S_2$ the emission cell was purged with argon and heated, and spectra were measured at 200 and 400 °C. The emission spectrum of crystalline MoO_3 was measured at 200 °C in argon. For sulfidation, MoO_3 was heated in a flow of 10% H_2S in H_2 and kept at the desired temperatures for 3 h. After purging the cell with argon, an emission spectrum was measured at the same temperature. Each spectrum is the sum of 500 scans, while the emission of the empty sample holder at 200 °C served as a background spectrum.

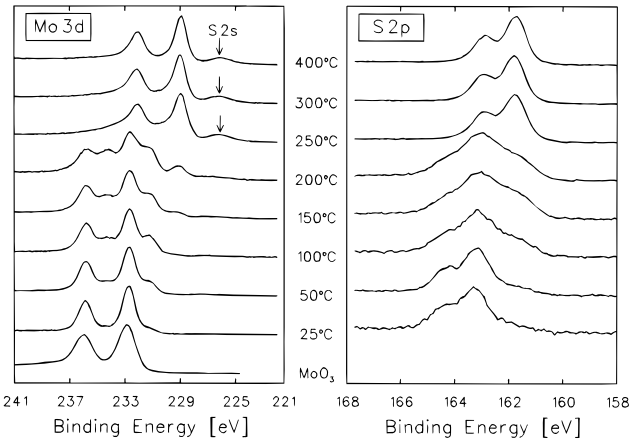

Figure 2. Mo 3d and S 2p XPS spectra of crystalline MoO_3 sulfided at the indicated temperatures for 3 h.

Results

The organization of this section is as follows. We first describe the XPS spectra of sulfided MoO_3, then the corresponding infrared spectra, and finally we describe the thermal decomposition of the $(NH_4)_2MoO_2S_2$ compound, which serves to provide references for local structures present in oxysulfides.

X-ray Photoelectron Spectroscopy of MoO_3 and Its Sulfidation Products. Figure 2 shows XPS spectra of MoO_3 after sulfidation in H_2S/H_2 at the indicated temperatures; binding energies are collected in Table 1; compositions are shown in Figure 3. The samples consisted of a thin layer of powder pressed in indium foil and possessed sufficient conductivity to prevent any buildup of charge, as judged from a single C 1s peak, which appeared at a constant binding energy of 284.6 ± 0.2 eV in all samples. The bottom spectrum of the Mo 3d series is that of the crystalline MoO_3. It consists of a single Mo 3d doublet with a Mo $3d_{5/2}$ binding energy of 232.9 eV, which is characteristic for molybdenum in a formal 6+ oxidation state.[13] Although sulfidation at lower temperatures already has a noticeable effect, the fully sulfided state appears to be reached at temperatures between 250 and 400 °C. Several intermediate situations emerge as well. We will first describe the spectrum of the fully sulfided sample.

The Mo 3d spectrum of the sample sulfided at 400 °C shows essentially one doublet with a Mo $3d_{5/2}$ binding energy of 229.0 eV, the expected value for the Mo^{4+} centers in MoS_2.[6,14] The corresponding S 2p spectrum consists of a single doublet with an S $2p_{3/2}$ binding energy of 161.8 eV, consistent with the S^{2-} type ligands present in MoS_2.[6,14]

The Mo 3d XPS spectra of the samples sulfided at intermediate temperatures (25−300 °C) can all be described in terms of the Mo^{6+} and Mo^{4+} doublets mentioned above and one additional doublet with a Mo $3d_{5/2}$ binding energy of 231.1 eV. This doublet is already present after sulfidation at room temperature, and we attribute it to Mo^{5+} present in oxysulfide intermediate phases. The Mo 3d spectra of the sulfided samples contain contributions of these three states in varying percentages, reflecting the stepwise transition of Mo^{VI} in MoO_3 to Mo^{IV} in MoS_2 (see also Figure 3). The most obvious trends are

TABLE 1: Parameters of the XPS Spectra of Figure 2

		Mo^{6+}		Mo^{5+}		Mo^{4+}		$S_{2,br}^{2-}$		S^{2-} [a]	
T [°C]	S/Mo	E_b [eV]	fraction [%]	E_b [eV]	fraction [%]	E_b [eV]	fraction [%]	E_b [eV]	fraction [%]	E_b [eV]	fraction [%]
MoO_3		232.9	100								
25	0.15	232.7	89	231.2	11			163.2	89	161.7	11
50	0.37	232.7	75	231.2	25			163.2	82	161.6	18
100	0.38	232.7	65	231.1	31	229.2	4	163.1	66	161.7	34
150	0.52	232.7	55	231.1	35	229.0	10	163.1	55	161.7	45
200	0.95	232.7	44	231.1	39	229.1	17	163.1	58	161.7	42
250	1.75	232.7	9	230.9	21	229.1	70	162.9	8	161.8	92
300	1.8	232.7	5	230.9	17	229.1	78			161.8	100
400	1.9			230.7	10	229.0	90			161.8	100

[a] S^{2-} and/or terminal S_2^{2-} (cf. text).

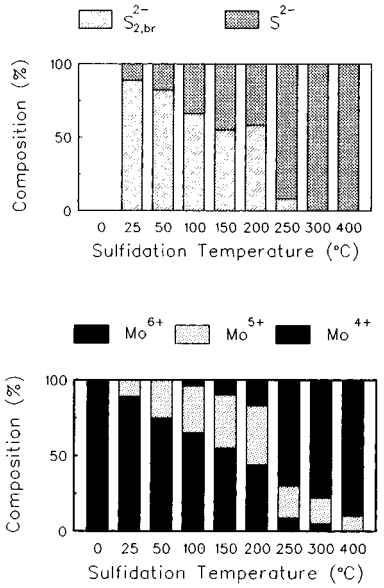

Figure 3. Composition of the XPS spectra of MoO_3 after 3 h of sulfidation, as a function of temperature.

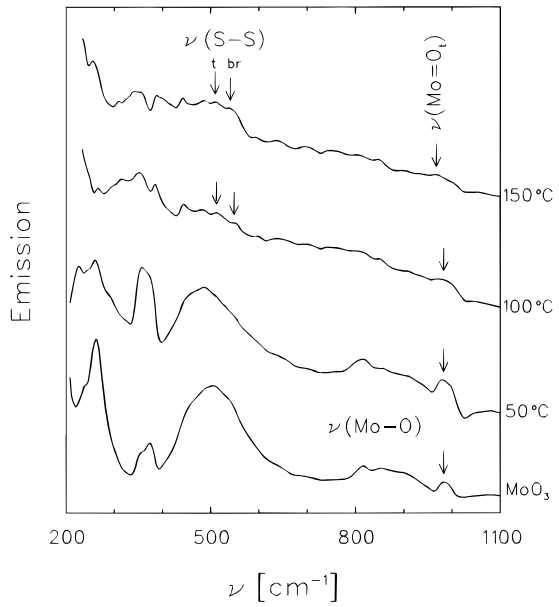

Figure 4. Infrared emission (IRE) spectra of crystalline MoO_3 sulfided at the indicated temperatures. Arrows indicate the position where contributions from terminal Mo═O_t groups (approximately 950 cm^{-1}) and S_2^{2-} ligands are expected.

increasing formation of Mo^{5+} centers at sulfidation temperatures below 200 °C and their reduction to the Mo^{4+} state at temperatures above 200 °C (Table 1).

The S 2p spectra of Figure 2 can all be interpreted in terms of two doublets only, with S $2p_{3/2}$ binding energies of 161.7 and 163.1 eV, respectively. We stress that the shifts in the spectra of Figure 2 have nothing to do with differential charging but are entirely caused by chemical changes in the samples. Using the S 2p XPS data of various Mo−S compounds as references,[5,6] we assign the peak at 163.1 eV to bridging disulfide (S_2^{2-}) ligands and the 161.8 eV peak to terminal disulfide *and/or* sulfide (S^{2-}) ligands. Note that terminal disulfide (S_2^{2-}) ligands can not be distinguished from sulfide (S^{2-}) ligands (as, for example, present in MoS_2) on the basis of XPS, although the formal oxidation state of sulfur is different. Figure 3 shows the contribution of the different molybdenum and sulfur states to the XPS spectra. The observation of signals due to reduced metal centers (Mo^{5+}) and oxidized sulfur ligands (S_2^{2-}) in the XPS spectra after sulfidation at low temperatures points to metal−ligand redox reactions as one of the first elementary reaction steps during sulfidation.

Infrared Emission Spectroscopy of MoO_3 and Its Sulfidation Products. The IRE spectrum of crystalline MoO_3 in Figure 4 shows several bands due to ν(Mo−O) and δ(Mo−O) vibrations.[15,16] The band at 985 cm^{-1}, indicated by an arrow in Figure 4, reflects the ν(Mo−O) stretch vibration of terminal $-Mo^{VI}$═O_t groups. The broad vibrational features between 800 and 900 cm^{-1} (i.e. 815, 850, and 895 cm^{-1}) are due to ν_s(Mo−O) vibrations of μ_3 and μ_2 bonded oxygen within the (a,b) and (b,c) planes of the MoO_3 lattice (see Figure 5 for the structure

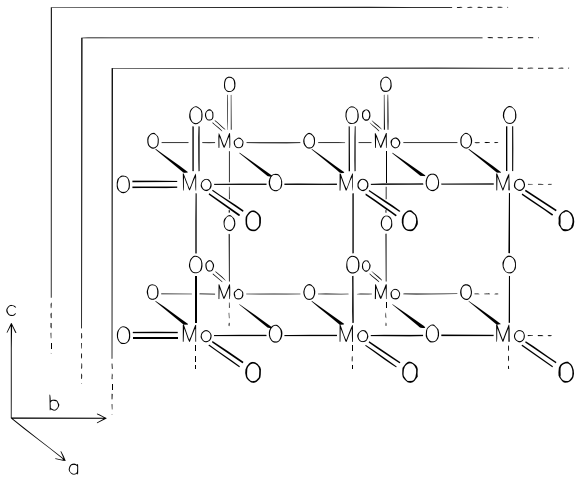

Figure 5. Structure of crystalline MoO_3. Layers are stacked along the *a*-axis.

of MoO_3). These Mo−O bonds possess bond orders varying between 1.7 and 0.3,[11] and hence the correspondingly varying force constants give rise to a broad band with unresolved contributions. The bands below 700 cm^{-1} are due to ν_{as}(Mo−O) and δ(Mo−O) vibrations.

The upper three traces of Figure 4 are the IRE spectra of MoO_3 after sulfidation in H_2S/H_2. The ν(Mo−S) and ν(S−S) vibrations come between 200 and 550 cm^{-1}, but the bands are relatively weak and they overlap with Mo−O deformation

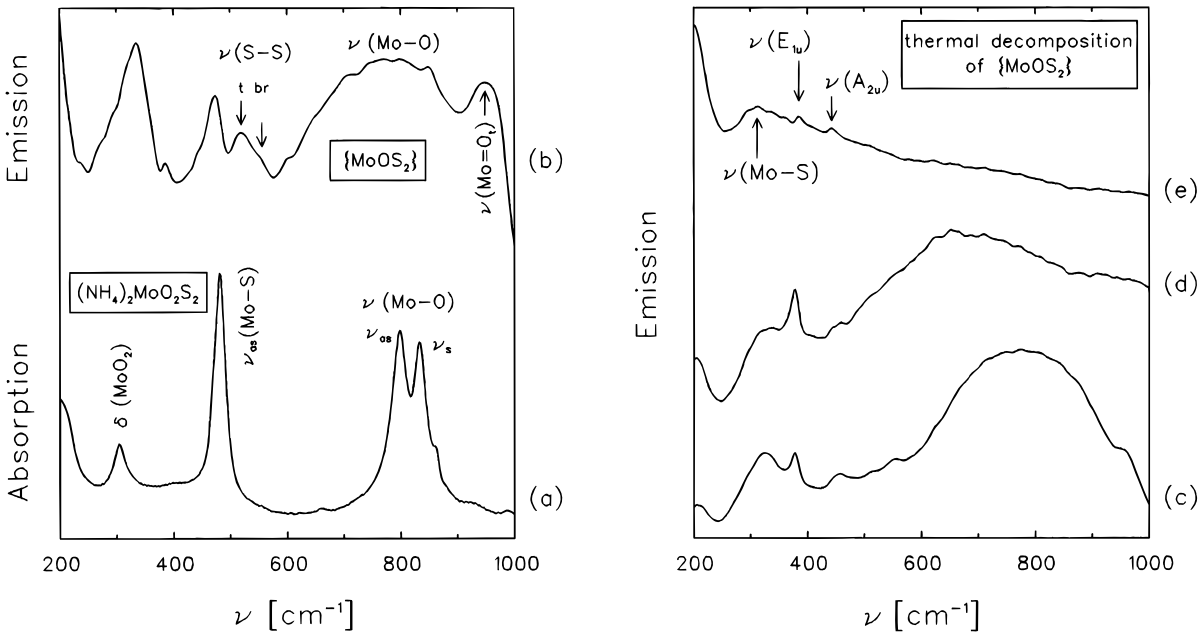

Figure 6. Absorption IR spectrum of $(NH_4)_2MoO_2S_2$ (a) and emission IR spectra at 200 °C (b) and 400 °C (c, d, e).

modes. As a result, the ν(Mo−O) vibrations between 750 and 1000 cm^{-1} give the most conclusive information on the change of the Mo−O coordination during sulfidation.

If we compare the spectra of the sulfided samples with that of MoO_3, two points can be noted. First, the signal characteristic of terminal Mo═O_t at 985 cm^{-1} increases upon sulfidation at 50 °C and decreases but remains detectable after sulfidation at higher temperatures, accompanied by a small shift to lower frequencies. Secondly, the broad band due to ν(Mo−O) vibrations of μ_2 and μ_3 bonded oxygen disappears before the Mo═O_t signal, indicating that the MoO_3 framework in the surface region largely collapses at temperatures below 100 °C. The characteristic bands due to the stretch vibrations of terminal and bridging S_2 groups come at 510 and 530 cm^{-1}, respectively, and have been indicated by arrows in Figure 4. Indeed, some emission is noticeable in this range, but the signal is weak as expected. Their presence is in agreement with the XPS spectra discussed above, which contain clear evidence for bridging S_2^{2-} groups in partially sulfided samples.

Assignment of bands below 500 cm^{-1} is not warranted, because δ(Mo−O) and ν(Mo−S) vibrations overlap. Spectra of samples after sulfidation at temperatures above 150 °C have been recorded but show weak features only and are not discussed. The spectrum of the fully sulfided sample is the same as that of the MoS_2 phase formed by thermal decomposition of $(NH_4)_2MoO_2S_2$ (Figure 6e), which we briefly discuss below. The important information from the infrared spectra is that additional terminal −Mo═O_t groups form during sulfidation of MoO_3 and that these are also the Mo−O entities that remain present in the oxysulfide stage, while configurations of the type Mo−O−Mo convert in earlier stages of the sulfidation.

Infrared Spectra of $(NH_4)_2MoO_2S_2$ and Its Thermal Decomposition Products. Interpretation of the infrared and XPS spectra of the partially sulfided samples is hindered by the unknown structure and poor definition of these oxysulfide phases. To obtain better interpretable data, which may serve as a reference case for the structures encountered in partially sulfided MoO_3-based catalysts, we have studied the complex $(NH_4)_2MoO_2S_2$. Upon heating, this compound decomposes via an oxysulfide phase of stoichiometry $\{MoOS_2\}$ to the thermodynamically stable sulfide MoS_2.[7] The infrared spectrum of the intermediate $\{MoOS_2\}$ phase reveals structural features that we expect to be generally characteristic for molybdenum oxysulfide structures.

TABLE 2: Bands in the IR Spectra of $(NH_4)_2MoO_2S_2$[17] and $\{MoOS_2\}$ (See Figure 6a,b)

$(NH_4)_2MoO_2S_2$ [cm^{-1}]	$\{MoOS_2\}$ [cm^{-1}]	assignment
	950	ν(Mo═O_t)
	850	ν(Mo−O)[a]
833		ν_s(Mo−O)
	805	ν(Mo−O)[a]
798		ν_{as}(Mo−O)
	770	ν(Mo−O)[a]
	710	ν(Mo−O)[a]
	548	ν(S−S)$_{br}$
	523	ν(S−S)$_t$
482		ν_{as}(Mo−S)
	472	ν(Mo−S)[b]
	386	ν(Mo−S)[b]
	334	ν(MoS)[b]
	334	δ(Mo−O−Mo)[b]
305		δ(MoO_2)
200		δ(MoS_2)

[a] ν(Mo−O) vibrations of Mo_x−O−Mo (x = 1, 2) functions. [b] ν(Mo−S) vibrations of Mo−$(S)_x$−Mo (x = 1, 2) functions.

The infrared absorption spectrum of $(NH_4)_2MoO_2S_2$ in Figure 6a shows the characteristic bands of the $MoO_2S_2^{2-}$ anion (see Table 2), as reported by Schmidt et al.[17] The $\{MoOS_2\}$ phase is known to form after heating to 200 °C; the corresponding infrared spectrum, measured in emission mode, is shown in Figure 6b. It contains several bands due to Mo−O and Mo−S vibrations (detailed assignments in Table 2). In short, the bands above 600 cm^{-1} correspond to Mo−O vibrations, and they indicate that oxygen is present in similar types of coordination as in MoO_3. We assign the band at 950 cm^{-1} to the ν(Mo−O) vibrations of terminal −Mo═O_t groups. The frequency of the ν(Mo═O_t) vibration is shifted 35 cm^{-1} to lower wavenumbers compared to its value in crystalline MoO_3, due to the presence of reduced Mo centers and sulfur as a ligand.

The broad band around 800 cm^{-1} is attributed to ν(Mo−O) vibrations of μ_2 and μ_3 bonded oxygen of Mo−O−Mo and Mo_2−O−Mo fragments. The large half-width of this band (≈200 cm^{-1}) shows that the Mo−O coordination includes a high degree of nonuniformity. In the case of simple dinuclear transition metal oxygen complexes, the ν_s and ν_{as}(M−O) vibration of M−O−M bridges cover a range of more than 300

cm^{-1} depending on the bonding angle.[18] We therefore conclude that the $\{MoOS_2\}$ phase exhibits a significant dispersion of Mo−O−Mo bond angles, which leads to a range of splittings between the symmetric and antisymmetric stretching modes.

The band at 523 cm^{-1} and its shoulder at 548 cm^{-1} in the spectrum of $MoOS_2$ in Figure 6b are due to the ν(S−S) vibrations of terminal and bridging S_2^{2-} ligands,[5] respectively. The presence of the latter shows that Mo centers are connected not only via oxygen but also via sulfur. The less characteristic bands at 472, 386, and 334 cm^{-1} are assigned to ν(Mo−S) vibrations of Mo−S−Mo and Mo−(S_2)−Mo[19] units, while the band at 334 cm^{-1} should also contain significant contributions of δ(Mo−O) deformation modes.

The occurrence of the S_2^{2-} ligands implies that at least some of the initial S^{2-} ligands in the $MoO_2S_2^{2-}$ anion have been oxidized during thermal decomposition ($2S^{2-} \rightarrow S_2^{2-} + 2e$). As a consequence, Mo centers must be present in the $\{MoOS_2\}$ phase in a formal oxidation state less than 6+. XPS spectra (not shown) indeed confirmed that the Mo $3d_{5/2}$ peak has a binding energy 2−3 eV lower than that of MoO_3, indicative of a 5+ or 4+ state. We note, however, that the XPS measurements of the $MoOS_2$ phase seriously suffered from inhomogeneous charging and sample decomposition during measurement. As a result, an accurate analysis of the peaks is not possible.

Upon heating to 400 °C, the $\{MoOS_2\}$ phase reacts further to microcrystalline MoS_2. Figure 6c−e shows emission infrared spectra after 30, 60, and 90 min at 400 °C, respectively. Significant spectral changes within the region due to Mo−O vibrations (600−1000 cm^{-1}) reveal that the terminal Mo═O_t groups at 950 cm^{-1} are the first to disappear under these conditions. Obviously, Mo═O_t fragments form the most labile part of the $\{MoOS_2\}$ phase. They are likely to convert by reductive elimination of O_2, such as

$$2 - Mo^{n+}{=}O_t \rightarrow 2 - Mo^{(n-1)+} + O_2$$

$$-Mo^{n+}(=O_t)_2 \rightarrow -Mo^{(n-2)+} + O_2 \qquad (5)$$

Simultaneously with the release of O_2, the intensity of the band at 330 cm^{-1}, which contains δ(Mo−O) contributions, decreases. In addition, the maximum of the broad band due to the ν(Mo−O) vibration of Mo_x−O−Mo ($x = 1, 2$) bridges shifts down to 680 cm^{-1} (Figure 6b). This may be due to an increasing coupling of ν(Mo−O) and ν(Mo−S) vibrations. After 90 min the decomposition reaction is completed and a microcrystalline MoS_2 phase has been formed. Its spectrum (Figure 6e) contains weak bands only. For reference, bands of the $\nu(A_{2u})$ and $\nu(E_{1u})$ phonons of crystalline MoS_2, which come at 470 and 384 cm^{-1} at room temperature, have been indicated.[20] The approximately 20 cm^{-1} shift of the $\nu(A_{2u})$ vibration to lower wavenumbers in the MoS_2 spectrum of Figure 6e can largely be attributed to the higher temperature of 400 °C at which the emission spectrum was taken.[21] However, the presence of the rather broad band around 320 cm^{-1} implies that the MoS_2 phase still includes imperfections regarding the arrangement of the sulfur planes. We address this point in the Discussion section.

The point to note is that during thermal decomposition of the compound $(NH_4)_2MoO_2S_2$ to oxysulfides, −Mo═O_t fragments (like in MoO_3) are formed at intermediate temperatures (200 °C). These groups disappear in the conversion of the intermediate to MoS_2 before the other Mo−O configurations do, indicating the relatively high reactivity of these Mo═O_t fragments.

Discussion

The most important results from this work can be summarized as follows.

(1) The initial sulfidation of MoO_3 results in the reduction of Mo^{6+} to Mo^{5+} and the oxidation of sulfide ligands to bridging S_2^{2-} ones (Figures 2 and 3).

(2) Bridging Mo−O−Mo configurations of the MoO_3 lattice disappear between 50 and 100 °C while additional terminal −Mo═O_t groups appear (Figure 4), indicating that the Mo−O−Mo structures break up to form terminal −Mo═O_t entities.

(3) The rapid disappearance of the terminal Mo═O_t groups during heating of the $\{MoOS_2\}$ model oxysulfide in the *absence* of H_2S while bridging Mo−O−Mo configurations disappear at a significantly lower rate (Figure 6b) indicates that terminal Mo═O_t are the most reactive oxygen-containing entities in oxysulfides.

In this section we combine the above findings with literature data on reactions of various molybdenum compounds to propose a molecular mechanism for the sulfidation of MoO_3. The XPS spectra and their decomposition in Figure 3 indicate that major changes in composition occur after sulfidation at temperatures above 200 °C, where the spectra become very much like those of MoS_2. Hence, the range between ambient temperature and somewhere between 200 and 250 °C is where oxysulfides prevail in sulfided MoO_3. Therefore, we first address the early stage in which MoO_3 is transformed into oxysulfides. Next we discuss structural properties of the model oxysulfide $\{MoOS_2\}$ and finally the conversion of the oxysulfide phase into MoS_2.

The Reaction of MoO_3 with H_2S to Oxysulfides (Room Temperature to 200 °C). The relative instability of the terminal Mo═O_t groups suggests that these entities play a dominant role in the uptake of sulfur. In fact, the exchange of oxygen for sulfur in terminal Mo═O_t has known occurrence in the solution chemistry, e.g. the reaction of molybdate with H_2S in NH_4OH to tetrathiomolybdate ($MoO_4^{2-} + 4H_2S \rightarrow MoS_4^{2-} + 4H_2O$). Depending on the concentration of the NH_4OH solution, the reaction may proceed via H_2S or SH^- (formed in situ by deprotonation of H_2S) as the reactive agents.[22,23] In the case of the sulfidation reaction such a deprotonation is not possible and H_2S must be considered as the reactive component:

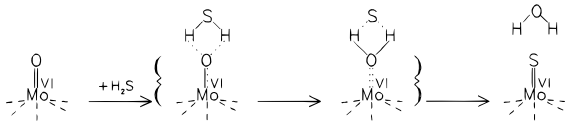

(6)

This particular type of interaction between H_2S and the −Mo═O_t fragment leads formally to a protonation of the O^{2-} ligand, which weakens the Mo═O as well as the S−H bonds; H_2O is already preformed in the transition state. Due to rotation of the $\{OH_2S\}$ arrangement, H_2O is released and an S^{2-} ligand remains at the Mo^{VI} center without a change of the coordination number during the whole reaction sequence. Terminal oxygen ligands located on the (a,b) and (a,c) planes of the MoO_3 crystal (see Figure 5) are accessible for this reaction. The thermodynamical driving force for reaction 6 is the formation of H_2O.

The reduction of Mo^{6+} to Mo^{5+} and the oxidation of S^{2-} from H_2S to bridging S_2^{2-} groups in the partially sulfided MoO_3 has been observed before in SiO_2-supported MoO_3 model catalysts[6] and has been explained by the following two elementary reaction steps:

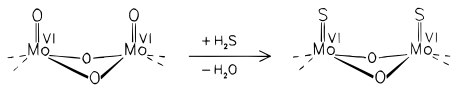

(7)

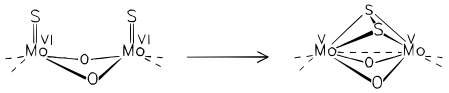

(8)

The first is reaction 6 on two adjacent sites. The second step involves a metal−ligand redox reaction in which two S^{2-} ligands, bonded to adjacent Mo^{VI} centers, are oxidized ($2S^{2-} \rightarrow S_2^{2-} + 2e$) while the metal centers are reduced ($2Mo^{VI} + 2e \rightarrow 2Mo^{V}$). The occurrence of the overall reaction of 7 and 8 is strongly supported by the XPS data of Figures 2 and 3 and is in agreement with the infrared spectra of Figure 4, where characteristic emission from disulfide species can be recognized.

The exchange of terminal oxygen ligands for the larger sulfur in the MoO_3 lattice is expected to have sterical consequences, especially within the (a,b) plane. Structural reorganization of the surface accompanies the redox process 8, as reduction of the metal centers lead to stronger metal−metal interactions, i.e. to shorter Mo−Mo distances. Taking the $[Mo_2S_{12}]^{2-}$ anion (d(Mo−Mo) = 282 pm[24]) as a model for an $\{Mo^{V}-Mo^{V}\}$ fragment, we expect the Mo−Mo distance (after reduction) to be between 282 and 300 pm, the latter being the distance of the relevant Mo centers within the (a,b) plane in MoO_3.[10] The shortening of the Mo−Mo distance places the metals closer to the center of the $[MoO_6]$ octahedra, and the three Mo−μ_3O bonds become more equivalent. The positions of the sulfur atoms change as well: The S−S vector of the formed S_2 unit is nearly perpendicular to the Mo−Mo vector.[9] Due to the structure of the MoO_3 (see Figure 5), the redox reaction 5 can only take place within the (a,b) plane and not within the (a,c) plane, where the Mo−Mo distance is as large as 396 pm.[10] This explains the presence of both bridging S_2^{2-} and terminal S^{2-} ligands and their relative intensities after sulfidation at 50 °C, as obtained from the XPS spectra (see Figure 3).

After sulfidation at 100 and 150 °C small amounts of Mo^{4+} were formed. Although a direct reaction between terminal O^{2-} ligands and H_2, formally according to

$$-Mo^{VI}{=}O_t + H_2 \rightarrow Mo^{IV} + H_2O \qquad (9)$$

cannot be excluded, we consider that in view of the relatively low temperature of 100−150 °C more likely an exchange and subsequent redox reaction occur at edge metal centers, with (formally) two terminal O^{2-} ligands:

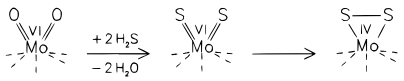

(10)

Direct reduction, i.e. reaction 9, is expected to become relevant at higher temperatures, with a considerably higher yield of Mo^{4+}. This has, in fact, been shown in the TPS measurements by Moulijn and co-workers on crystalline MoO_3,[2] which show intense H_2 consumption and H_2O production peaks at ca. 350 °C, i.e. about 200 °C higher than where the first Mo^{4+} arises in the XPS spectra (Figures 2 and 3). We therefore propose that at 100−150 °C small amounts of Mo^{4+} may form through reaction 10, with the simultaneous formation of terminal S_2 groups, which are indeed visible in the corresponding IRE spectra of Figure 4 (band at 510 cm^{-1}).

An interesting feature of the sample after sulfidation at 100 °C is that while the XPS S/Mo ratio (0.38) is the same as after sulfidation at 50 °C (0.37), the relative amount of the respective sulfur ligands changed. Visual inspection of the 100 °C S 2p spectrum in Figure 2 and the corresponding compositions in Figure 3 shows that the fraction of S^{2-} (and/or terminal S_2^{2-}) ligands increased at the expense of the bridging S_2^{2-} ligands. At the same time, the proportion of Mo in the 5+ state increased, as opposed to the contribution of bridging S^{2-} ligands. This suggests that between 50 and 100 °C sulfur has been released from the S_2 bridges, for which we propose the following reaction sequence:

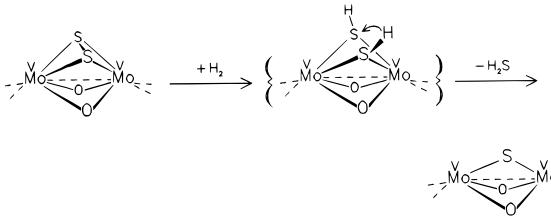

(11)

The first step is a reaction of the S_2 entity with H_2 to form two transient SH^- fragments. Stabilization of the SH^- ligands is unlikely, it would require a rigid stereochemistry brought about by bulky ligands and sufficient electron density on the metal centers. For example, the μ_2 SH^- ligands in the Mo^{IV} complex $MeCp\{Mo^{IV}(\mu_2S^{2-})_2(\mu_2SH^-)_2Mo^{IV}\}CpMe$ ($MeCp = CH_3C_5H_4$)[25] could be prepared from bridging S_2 entities by reaction with H_2 at room temperature. In the present case, however, there are no bulky ligands available for kinetic stabilization. Furthermore, the relatively low electron density weakens the S−H bond and increases the acidity of the SH^- ligand. Stabilization is readily achieved by proton transfer, forming an H_2S complex, which decomposes immediately, similarly as described by Müller and Diemann.[9] At higher temperatures (400 °C) both sulfur atoms of the S_2 entity react under formation of coordinatively unsaturated Mo centers.[8]

The release of sulfur from S_2 units reduces the sterical hindrance on the surface of the crystal and gives space for the formation of new S_2 groups according to (7) and (8), which is reflected in a higher S/Mo ratio in the XPS spectrum of the sample sulfided at 150 °C (Table 1). The low intensity of the band due to the $\nu(Mo{=}O_t)$ vibration in the corresponding IRE spectrum implies that most of the available $Mo{=}O_t$ functions have reacted at 150 °C. The sulfur content increases further after sulfidation at 200 °C, which is close to the temperature up to which oxysulfides prevail.

Structural Properties of the $\{MoOS_2\}$ Oxysulfide. The thermal decomposition of $(NH_4)_2MoO_2S_2$ at 200 °C in inert gas leads to the formation of an amorphous phase of stoichiometry $MoOS_2$ (reaction 2). Some of the steps in the decomposition bear resemblance to the formation of MoS_3 from $(NH_4)_2MoS_4$, which we published recently.[5] The first elementary reaction step in (2) is a proton transfer from the two NH_4^+ cations to an O^{2-} ligand of the $MoO_2S_2^{2-}$ anion, producing NH_3 and a neutral $\{S_2MoOH_2O\}$ intermediate. The latter is not stable and aggregates. The IR emission spectrum of Figure 6b reveals that this $\{MoOS_2\}$ phase possesses Mo_x-O-Mo ($x = 1, 2$), Mo−(S_2)−Mo, and very likely Mo−S−Mo linkages. Corresponding vibrational features were present in the infrared spectra of partially sulfided MoO_3 as well. The most remarkable and important characteristic of the amorphous $\{MoOS_2\}$ phase, however, is that it contains a significant amount of oxygen in terminal positions, $Mo{=}O_t$, as indicated by the strong band at 950 cm^{-1} in Figure 6b. Such groups are not present in the initial $(NH_4)_2MoO_2S_2$. Since the $\{MoOS_2\}$ phase has been formed within a simple thermal decomposition where no special reaction conditions have been applied, we infer that the presence of O^{2-} ligands in bridging and terminal positions is a common structural property of oxysulfides. Again, the terminal O^{2-} are the most reactive ones within this phase; if the temperature is increased, they are the first to convert (Figure 6c−e). Apparently, the $Mo{=}O_t$ functions are essential for coordinative saturation of metal centers in the oxysulfide, but they are released if the temperature is high enough to form the stable MoS_2 structure in inert gas atmosphere. The $\{MoOS_2\}$ phase is not expected to be stable in the H_2/H_2S mixture, because the $Mo{=}O_t$ functions would immediately react after they have been formed.

The structure of the oxysulfides formed during sulfidation of MoO_3 at 150−200 °C is far from thermodynamical equilib-

rium, for several reasons. The saturation of the surface with sulfur and the generation of reduced metal centers distorts the structure, especially in the surface−bulk interface area. While MoS_2 is already the equilibrium solid state structure for the surface region in this stage, it is still MoO_3 for the bulk. This, together with the increased mobility at 200 °C, may well cause the oxysulfide structure to break up, whereby new terminal O^{2-} ligands form out of Mo_x−O−Mo ($x = 1, 2$) bridges (two of the Mo−O bonds in each [MoO_6] octahedra are extremely weak). Immediately after their formation, the Mo═O_t groups will react as described above (reactions 7 and 8 and also 9). In this stage there is still an approximate correlation between the amount of Mo^{5+} centers and bridging S_2^{2-} ligands.

Reaction of Oxysulfides with H_2S to MoS_2 (200−400 °C). Sulfidation of MoO_3 at temperatures above 200 °C results in a major change in composition as compared to that of the oxysulfides formed at lower temperatures. Mo^{6+} and Mo^{5+} have largely reduced to Mo^{4+}, and the contribution of bridging S_2^{2-} to the S 2p spectra has virtually disappeared (Figure 3). The formation of Mo^{4+} is, in agreement with TPS data of Moulijn and co-workers,[2] mainly attributed to a reaction of −Mo═O_t with H_2 according to (9), and the subsequent uptake of sulfur from the sulfiding atmosphere, until eventually MoS_2 forms. Reductive elimination of terminal S_2^{2-} ligands (formation according to reaction 10) together with subsequent reduction of bridging S_2^{2-} to S^{2-} ligands as discussed by Muijsers et al.[6] is unlikely here. This type of reaction typically decreases the S/Mo ratio at higher temperatures, which is not observed here (Table 1).

The infrared emission spectra of MoS_2 phases obtained either by sulfidation of MoO_3 at 400 °C or by decomposition of $(NH_4)_2MoO_2S_2$ (see Figure 6e) give evidence for imperfections in the arrangement of the sulfur planes of MoS_2. The spectra contain a broad band around 320 cm^{-1}, which is absent in the spectrum of crystalline MoS_2.[26] In a phase containing Mo^{4+} and S^{2-} such bands around 320 cm^{-1} are usually assigned to ν(Mo−S) vibrations of μ_2 S^{2-} ligands, in Mo−S−Mo configurations.[27,28] The presence of this band suggests that some of the S^{2-} ligands are disordered and not (yet) part of the MoS_2 lattice. It is conceivable that during structural reorganization or aggregation small regions of MoS_2 are formed, which are interconnected by Mo−S−Mo bridges, as, for example, in structure **1**.

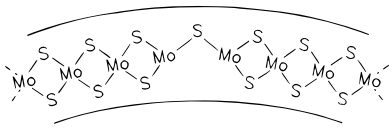

1

This type of defect goes along with a deficiency of sulfur and leads to a bending of the MoS_2 layer, which in fact has been observed with transmission electron microscopy.[6,29] Also the decomposition of MoS_3 as followed in situ in the TEM, leads to the formation of bent MoS_2 layers.[30] Formation of a perfect MoS_2 lattice would require much higher temperatures of about 800 °C.[31] Hence, the sulfidation of MoO_3 at temperatures typically employed in catalyst pretreatments (about 400 °C) leads to a microcrystalline MoS_2 phase, relatively rich in defects.

Concluding Remarks

The aim of this study was to study the sulfidation of crystalline MoO_3 to get a better understanding of the sulfidation mechanism of molybdenum oxides, which is an essential step in the activation of hydrotreating catalysts. Because there are significant differences between the structure and the properties of highly dispersed oxidic precursors in catalysts and crystalline MoO_3, particularly with respect to the extent of (de)hydration, the present work on the sulfidation of crystalline, dehydrated MoO_3 provides a useful reference case for understanding the sulfidation reaction in the more complex systems such as supported catalysts, which we discuss in a forthcoming paper on $MoO_3/SiO_2/Si(100)$ model catalysts.[32]

Acknowledgment. We gratefully acknowledge the skillful assistance of M. van Gorp, Th. M. Maas, and Ir. P. Brinkgreve from the Central Technical Workshops at the Eindhoven University of Technology and of W. van Herpen from our own department in the construction of the infrared emission cell. Valuable discussions with Dr. E. Diemann (Bielefeld), Dr. V. H. J. de Beer, and Prof. Dr. J. A. R. van Veen (Eindhoven) are gratefully acknowledged.

References and Notes

(1) Prins, R.; de Beer, V. H. J.; Somorjai, G. A. *Catal. Rev.-Sci. Eng.* **1989**, *31*, 1.
(2) Arnoldy, P.; van den Heijkant, J. A. M.; de Bok, G. D.; Moulijn, J. A. *J. Catal.* **1985**, *92*, 35.
(3) Scheffer, B.; Arnoldy, P.; Moulijn, J. A. *J. Catal.* **1988**, *112*, 516.
(4) de Jong, A. M.; Borg, H. J.; van IJzendoorn, L. J.; Soudant, V. G. F. M.; de Beer, V. H. J.; van Veen, J. A. R.; Niemantsverdriet, J. W. *J. Phys. Chem.* **1993**, *97*, 6477.
(5) Weber, Th.; Muijsers, J. C.; Niemantsverdriet, J. W. *J. Phys. Chem.* **1995**, *99*, 9194.
(6) Muijsers, J. C.; Weber, Th.; van Hardeveld, R. M.; Zandbergen, H. W.; Niemantsverdriet, J. W. *J. Catal.* **1995**, *157*, 698.
(7) Prasad, T. P.; Diemann, E.; Müller, A. *J. Inorg. Nucl. Chem.* **1973**, *35*, 1895.
(8) Diemann, E.; Weber, Th.; Müller, A. *J. Catal.* **1994**, *148*, 288.
(9) Müller, A.; Diemann, E. In *Comprehensive Coordination Chemistry*; Wilkinson, G., Gillard, R. D., McCleverty, J. A., Eds.; Pergamon: Oxford, 1987; Vol. II, Chapter 16.1.
(10) Hulliger, F. *Structural Chemistry of Layer-Type Phases*; Lévy, F., Ed.; D. Reidel Publishing Co.: Dordrecht, 1976.
(11) Pope, M. T. *Prog. Inorg. Chem.* **1991**, *39*, 181.
(12) McDonald, J. W.; Delbert Friesen, G.; Rosenheim, L. D.; Newton, W. E. *Inorg. Chim. Acta* **1983**, *72*, 205.
(13) Barr, T. L. *J. Phys. Chem.* **1978**, *82*, 1801.
(14) Patterson, T. A.; Carver, J. C.; Leyden, D. E.; Hercules, D. M. *J. Phys. Chem.* **1976**, *80*, 1702.
(15) Primet, M.; Fouilloux, P.; Imelik, B. *Surf. Sci.* **1979**, *85*, 457.
(16) Hewett, W. D., Jr.; Newton, J. H.; Weltner, W., Jr. *J. Phys. Chem.* **1975**, *79*, 2640.
(17) Schmidt, K. H.; Müller, A. *Spectrochim. Acta, Part A* **1972**, *28*, 1829.
(18) Cotton, F. A.; Wing, R. M. *Inorg. Chem.* **1965**, *4*, 867.
(19) Müller, A.; Jaegermann, W.; Enemark, J. H. *Coord. Chem. Rev.* **1982**, *46*, 245.
(20) Wieting, T. J. *Solid State Commun.* **1973**, *12*, 931.
(21) Müller, A.; Weber, Th. *Appl. Catal.* **1991**, *77*, 243.
(22) Aymonino, P. J.; Ranade, A. C.; Diemann, E.; Müller, A. *Z. Anorg. Allg. Chem.* **1969**, *371*, 300.
(23) Harmer, M. A.; Sykes, A. G. *Inorg. Chem.* **1980**, *19*, 2881.
(24) Müller, A.; Nolte, W.-O.; Krebs, B. *Angew. Chem.* **1978**, *90*, 286.
(25) Casewit, C. J.; Coons, D. E.; Wright, L. L.; Miller, W. K.; Rakowski Du Bois, M. *Organometallics* **1986**, *5*, 951.
(26) Wieting, T. J.; Verble, J. L. *Phys. Rev. B* **1971**, *3*, 4286.
(27) Müller, A.; Jostes, R.; Eltzner, W.; Nie, C. S.; Diemann, E.; Bögge, H.; Zimmermann, M.; Dartmann, M.; Reinsch-Vogell, U.; Che, S.; Cyvin, S. J.; Cyvin, B. N. *Inorg. Chem.* **1985**, *24*, 2872.
(28) Weidlein, J.; Müller, U.; Dehnicke, K. *Schwingungsfrequenzen II*; Georg Thieme Verlag: Stuttgart, New York, 1986.
(29) Datye, A. K.; Smith, D. J. *Catal. Rev.-Sci. Eng.* **1992**, *34*, 129.
(30) Weber, Th.; Zandbergen, H. W.; Niemantsverdriet, J. W. To be published.
(31) van Arkel, A. E. *Recl. Trav. Chim. Pays-Bas.* **1926**, *45*, 442.
(32) Weber, Th.; Muijsers, J. C.; Handels, F. J. A.; de Beer, V. H. J.; van Veen, J. A. R.; Niemantsverdriet, J. W. To be published.

JP961204Y